Optical absorption in epitaxial $La_{1-x}Sr_xFeO_3$ thin films

M D. Scafetta, Y. J. Xie, M. Torres, J. E. Spanier, and S. J. May[a)]
Department of Materials Science and Engineering, Drexel University, Philadelphia, Pennsylvania 19104, USA

(Received 1 February 2013; accepted 19 February 2013; published online 28 February 2013)

We report the dependence of optical absorption on Sr concentration in $La_{1-x}Sr_xFeO_3$ (LSFO) ($x \leq 0.4$) perovskite thin films. Strained epitaxial films were deposited on $SrTiO_3$ substrates using oxide molecular beam epitaxy. We find systematic changes in the optical absorption spectra with increasing x including a red-shift of transition energies and the increasing presence of a lower energy transition within the fundamental gap of pure $LaFeO_3$. These results serve as a demonstration of the complex manner in which absorption spectra can be altered in complex oxides via heterovalent *A*-site substitution. © *2013 American Institute of Physics*. [http://dx.doi.org/10.1063/1.4794145]

Perovskite oxides have become the subject of intense research efforts owing to their remarkable diversity of physical properties. Properties such as, but not limited to, superconductivity, ferroelectricity, and magnetism can be observed, tuned, and sometimes combined in perovskite oxide heterostructures.[1] Recently, there has been increased interest in engineering the optical properties of complex oxides for use in solar energy conversion and multifunctional optoelectronics.[2–6] However, unlike traditional compound semiconductors, there have been few systematic studies of how optical absorption spectra evolve with composition in quaternary perovskites.[7–11] The studies that have been reported highlight the need for systematic, experimental work, as optical band gaps and absorption spectra can exhibit a non-linear dependence on the material composition.[10,11] Such non-linearities may be particularly important in the case of non-d^0 perovskites, such as ferrites and manganites, which exhibit complex phase diagrams with electron correlations playing a major role in the electronic structure.

The material system $La_{1-x}Sr_xFeO_3$ (LSFO) is an interesting candidate for optical studies because of the vastly different ground states exhibited by the parent compounds $LaFeO_3$ (LFO) and $SrFeO_3$ (SFO). In the bulk, LFO exhibits a band gap of 2.1 eV,[12] while SFO is metallic.[13] In addition to the disparate electronic behavior of the parent compounds, which makes the system a promising one in which to tune optical transitions, the LSFO system exhibits a range of properties such as antiferromagnetism,[14,15] charge ordering,[16,17] and pressure- and field-induced magnetic transitions[18,19] that may find use in electronic or optoelectronic devices. Previous studies of LSFO have utilized x-ray-based spectroscopies to investigate alloying-induced changes in the electronic structure.[13,20–25] However, a systematic understanding is lacking regarding how optical properties change with *A*-site cation substitution in the LSFO system. In this letter, we report the synthesis and optical characterization of a set of $La_{1-x}Sr_xFeO_3$ ($x \leq 0.4$) films. Increasing the Sr concentration induces several systematic changes in the spectra including a red-shift of the lowest energy absorption edge in LFO. Additionally, an increase in absorption at energies below the LFO band gap is observed with Sr alloying, consistent with the formation of a Sr-induced state above the Fermi level, indicating that heterovalent *A*-site substitution produces a complex response in the absorption spectrum as opposed to a simple shifting of the band gap.

Thin films of LSFO were grown using oxide molecular beam epitaxy (MBE) (Omicron modified LAB-10 system). The metallic cations were sublimed or evaporated from elemental sources, the flux from which was measured using a quartz crystal monitor that was calibrated via Rutherford backscattering spectroscopy and x-ray reflectivity. Single crystal STO (001) substrates were used for the deposition of each sample. The substrates were etched for 30 s in aqua regia then annealed for 2 h at 1000 °C. Typical substrate temperatures ranged from 625 to 750 °C during deposition. Metal cations were co-evaporated, with each unit cell followed by a 20-30 s pause. The LFO films were grown in an O_2 or O_2/O_3 environment (approximately 5% O_3 in O_2), while all the LSFO films were grown using the ozone/oxygen mixture with a chamber pressure of 2.0×10^{-6} Torr. All films are 25-55 nm thick. The error in the cation stoichiometry (x) of the films is estimated to be roughly ± 0.03, based on drifting of the effusion cell flux during growth and the accuracy of flux calibration. Crystal growth was monitored *in situ* using reflection high energy electron diffraction (RHEED). *Ex situ* post-growth anneals were carried out in an oxygen tube furnace for 4 h at 650 °C under flowing O_2 to reduce oxygen vacancies.

X-ray diffraction and reflectivity was measured using a Rigaku SmartLab diffractometer to probe the crystalline quality, surface roughness, and thickness of the samples. The reflectivity data were fit using the GENX program[26] to determine film thickness and roughness. The *c*-axis lattice parameters were obtained by comparing the measured data and diffraction simulations using GENX, which can be seen in supplementary Figure S1.[27] High resolution diffraction and reciprocal space maps (Figs. 1(a) and 1(c)) were obtained from the Advanced Photon Source at Sector 33-BM. Optical properties of the films were measured at room temperature over the energy range of 1.25-5 eV using a J.A. Woolam M-2000U variable angle spectroscopic ellipsometer. Ellipsometry was carried out at five angles from 65°–75° to create a well-defined sample set for the fitting software. The ellipsometry data were fit using Film Wizard 32 software to extract the index of refraction (n) and the extinction coefficient (k) of the

a)Electronic mail: smay@coe.drexel.edu.

 © 2013 American Institute of Physics

Downloaded 28 Feb 2013 to 129.25.34.167. Redistribution subject to AIP license or copyright; see http://apl.aip.org/about/rights_and_permissions

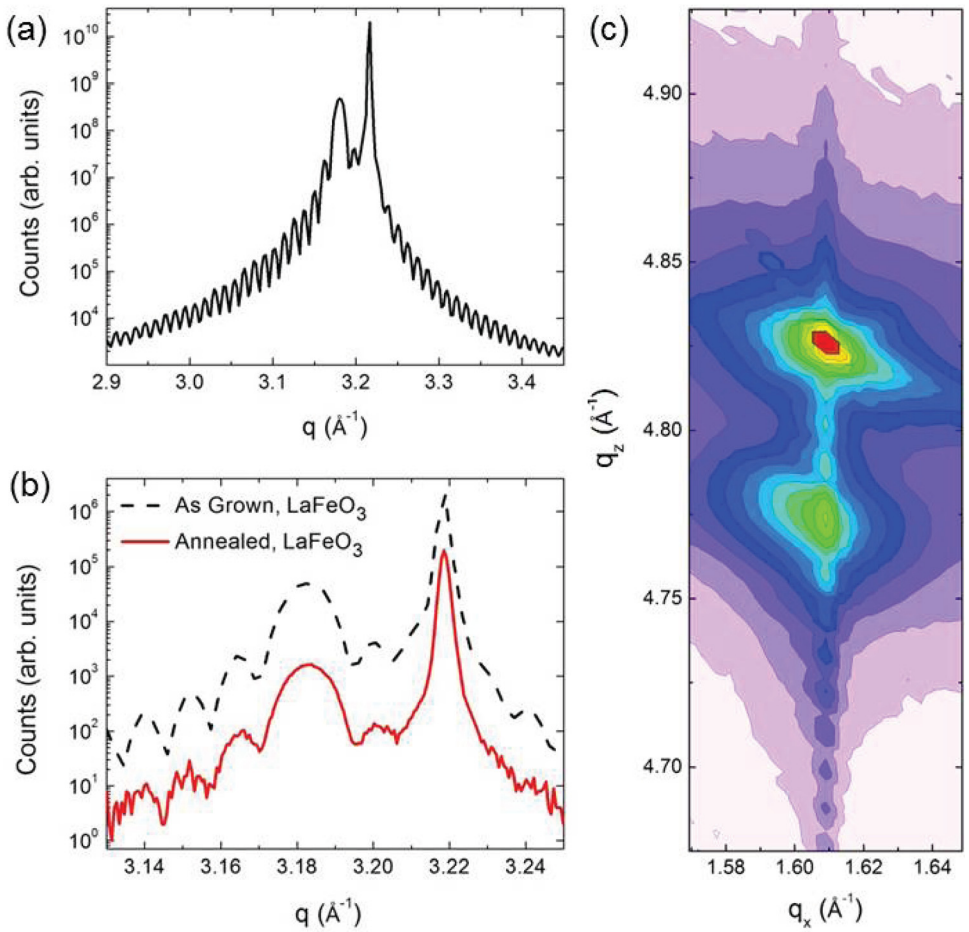

FIG. 1. High resolution x-ray diffraction data taken for a 49.9 nm LFO film grown on STO (001) (a)-(c). The (002) Bragg peak is shown in (a) and (b). The diffraction patterns in (b) compared before (dashed line) and after (solid line) post-growth annealing; no change is observed. A reciprocal space map of the (113) reflection of the as-grown film is shown in (c), confirming the film is coherently strained.

film from the film-substrate stack. The optical constants of the films were modeled using a series of Lorentz-Drude oscillators, with the thickness fixed at the value obtained from x-ray reflectivity. Optical absorption was determined using the relationship $\alpha = 4\pi k\lambda^{-1}$, where α is the absorption coefficient and λ is the incident photon wavelength.

Ternary LFO films are found to have a wide stability regime in terms of chamber growth pressure and substrate temperature. Figure 1(a) displays x-ray diffraction data obtained from a LFO film grown at 1×10^{-8} Torr. Scans over a wider q-range reveal only the specular (00 L) peaks, confirming that the film is phase pure with only a single out-of-plane crystallographic orientation. Similar results are obtained for films grown at pressures up to 5×10^{-6} Torr, which is the highest pressure used in this study. The films exhibit c-axis lattice parameters of 3.95 Å, consistent with the previous reports of LFO on STO.[28] Following growth, the film was annealed in flowing oxygen. X-ray diffractions measured before and after the anneal are given in Fig. 1(b). Unlike Sr containing films, as will be discussed below, negligible changes in the diffraction pattern were observed suggesting the LFO is fully oxidized in the as-grown state. Additionally, LFO films grown in either O_2 or an O_2/O_3 mixture yielded the same lattice constants. Figure 1(c) shows a reciprocal space map of the same film confirming the fully strained nature of the film.

In contrast, films containing Sr are found to be oxygen deficient when grown under similar conditions. Figure 2(a) presents the (002) diffraction peak measured from an as-grown $La_{0.6}Sr_{0.4}FeO_3$ film that was deposited at 2×10^{-6} Torr. The diffraction peak from the same film measured after a post-growth oxygen anneal is also presented. The c-axis parameter shifts from 3.934 Å to 3.896 Å following the anneal. Further annealing does not result in a continued decrease of the lattice parameter. The decreased lattice parameter is consistent with a reduction of oxygen vacancies. The presence of oxygen vacancies leads to an enhanced concentration of Fe^{3+} cations and a decreased concentration of Fe^{4+} cations. As the ionic radius of Fe^{3+} is larger than Fe^{4+}, the oxygen vacancies act to expand the lattice. Even compositions with relatively small amounts of Sr ($x \approx 0.08$) require post-growth annealing in oxygen to remove oxygen vacancies. As can be seen in Figures 2(b) and 2(c), the lattice parameters of the annealed LSFO films decrease monotonically with increasing substitution of Sr for La. For comparison, previously reported lattice constants[28–30] for LSFO thin films on STO (001) are also plotted in Figure 2(c) and are in good agreement with our results. Further confirmation of the film stoichiometry comes from variable temperature resistivity measurements (not shown), from which we obtain similar resistivity values compared to the bulk single crystals,[31] suggesting that the films are fully oxygenated after the anneal.

The room temperature optical absorption spectra for all samples were obtained using variable angle spectroscopic ellipsometry. The films were modeled as homogeneous smooth films on an infinite substrate. Prior to growth, each substrate was measured with ellipsometry to ensure accurate representation of the substrate contribution to the spectra measured from the films. The data were fit with a series

Downloaded 28 Feb 2013 to 129.25.34.167. Redistribution subject to AIP license or copyright; see http://apl.aip.org/about/rights_and_permissions

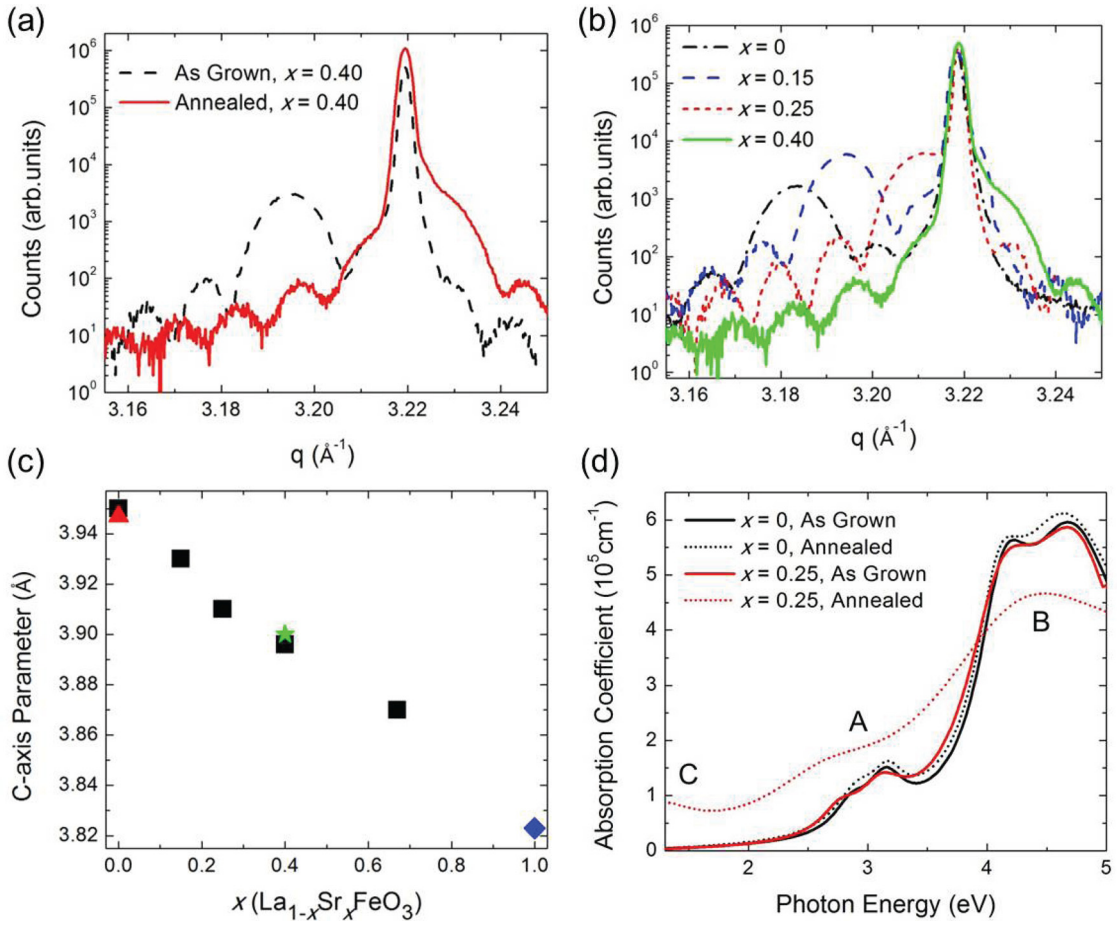

FIG. 2. Diffraction data obtained from the as-grown (dashed line) $La_{0.6}Sr_{0.4}FeO_3$ film and after annealing the same film (solid line) are presented in (a). The diffraction pattern for annealed films of varying composition is shown in (b). The out-of-plane lattice parameters are plotted against composition in (c). Data from the literature are included for comparison; the red triangle, green star, and blue diamond are from Refs. 28–30, respectively. A comparison of the optical absorption spectra between as-grown and annealed LFO and $La_{0.75}Sr_{0.25}FeO_3$ films is shown in (d). While negligible changes are observed in the LFO, the $La_{0.75}Sr_{0.25}FeO_3$ film exhibits a distinct change in the absorption after annealing induced by the removal of oxygen vacancies.

of Lorentz-Drude oscillators using a global modified Levenberg-Marquart algorithm. This process yielded the best fits on average for each film.

The Lorentz-Drude dielectric oscillator model follows the functional form,

$$\tilde{\epsilon} = \epsilon_\infty \left(1 + \sum_{j=1}^{m} \frac{A_j^2}{(E_C^2)_j - E(E - i\Gamma_j)} - \frac{\omega_P^2}{E(E + i\nu)}\right), \quad (1)$$

where ϵ_∞ is the high frequency dielectric constant, E_C is the center energy of the given oscillator, A is the oscillator amplitude fitting parameter, E is the incident photon energy, Γ is the broadening or vibrational fitting parameter, ω_P is the plasma frequency, and ν is the collision frequency. The obtained fitting parameters for the LSFO films are given in Supplementary Table S1.[27] Films containing Sr required four oscillators to achieve good RMSE values. In each case, one of these oscillators falls outside the measured region on the high energy side of the spectrum. For pure LFO, five oscillators were required. For LFO, the center energy of the oscillators is in good agreement with the similar material $BiFeO_3$ (BFO) with the exception of the small oscillator at 2.46 eV found in BFO but not LFO.[32]

The absorption spectrum for LFO is presented in Fig. 2(d). Negligible differences are observed in the spectra for the as-grown and post-growth annealed film, consistent with the previous conclusion that the as-grown LFO films are oxygen stoichiometric. In Sr-containing films, substantial changes to the absorption spectra are induced through the post-growth anneal process, as shown in Fig. 2(d) for the

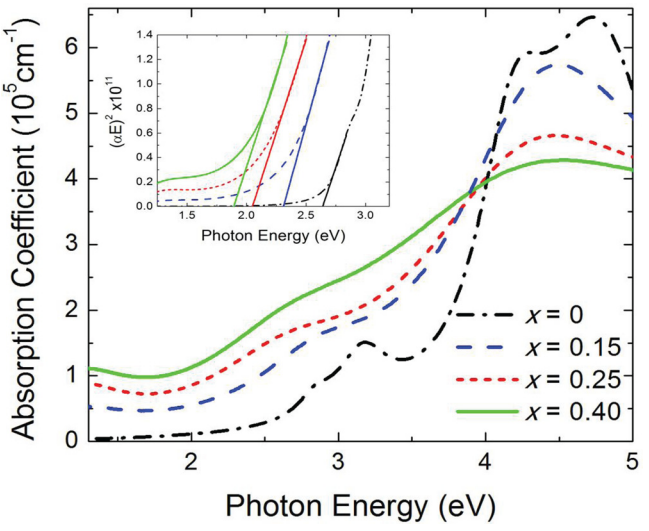

FIG. 3. Optical absorption spectra for the series of LSFO films. The inset shows the Tauc plots used in determining the energy for transition "A."

Downloaded 28 Feb 2013 to 129.25.34.167. Redistribution subject to AIP license or copyright; see http://apl.aip.org/about/rights_and_permissions

$x = 0.25$ film. In particular, the absorption spectra of the oxygen-deficient as-grown LSFO films are similar to the LFO films, while the oxygen anneal leads to changes in the absorption spectra that are systematically dependent on Sr concentration, as will be discussed below.

Based on previous work,[12,22,23] we attribute the transition labeled "A" in Fig. 2(d) to the electronic band gap for LFO. This transition corresponds to an excitation of electrons from a valence band consisting of hybridized Fe e_g majority spin and O $2p$ states to a conduction band comprised of primarily Fe $3d$ t_{2g} minority spin states. The energy gap for this transition was previously reported to be ≈2.1 eV for bulk LFO;[12] however, it is unknown if this transition is direct or indirect. In order to quantify the band gap, we follow the procedure used for many similar perovskite oxide materials (including BFO),[7,11,33,34] in which Tauc plots are employed to determine transition energies using the equation, $(\alpha E)^2 = (E - E_G)$, where α is the absorption coefficient, E is the incident photon energy, and E_G is the transition gap energy. The transition energy is obtained from the x-intercept of the $(\alpha E)^2$ vs. E plot. We obtain an optical band gap of 2.64 eV for the LFO film shown in Fig. 3. In total, we measured 4 LFO films and observed band gaps ranging from 2.63 to 2.67 eV. These values are slightly larger than that previously reported for bulk material (2.1 eV).[12] However, in the previous study, the band gap was obtained from the linear intercept of the optical conductivity derived from optical reflectivity data using bulk polycrystal samples. When using this method to determine band gap, in which we calculate optical conductivity from the extinction coefficient and refractive index, we obtain values around 2.45 eV for LFO. In addition to transition "A," there is a second absorption edge ("B") that has a transition energy of 3.85 eV as determined from Tauc analysis. This transition is attributed to the excitation of carriers from the valence band to unoccupied minority spin e_g states.[22]

Substitution of Sr for La induces several systematic changes in the optical absorption spectra. The transition labeled "A," the band gap in LFO, is red-shifted as seen in Fig. 3. The transition energy of this edge was fit using the direct gap Tauc method, shown in the inset of Fig. 3. Figure 4 displays a systematic reduction in the energy of transition "A" with increasing Sr content. From Fig. 4, it is clear that the energy of this transition will not extrapolate to 0 eV as expected for the parent compound SFO. Instead, an additional transition, labeled "C," can be seen emerging at energies below transition "A." Transition "C" is a result of a state forming within the gap of LFO as holes are added into the valence band.[22,23] Since this transition occurs at lower energies than the band gap for LFO, transition "C" likely represents the true band gap transition in Sr containing films. Unfortunately, our measurements do not capture the onset of transition "C," which is below the energy range of the ellipsometer. Thus, determining how the band gap changes as a function of strontium doping requires lower energy analysis than is reported here. However, our measurements reveal a simultaneous decrease of spectral weight in feature "B" and an increase in feature "C" with increasing x. This observation supports previous results suggesting that Sr alloying induces a transfer of electronic states from the valence band to a state above the Fermi level, likely derived from unoccupied e_g majority spin states.[22,23]

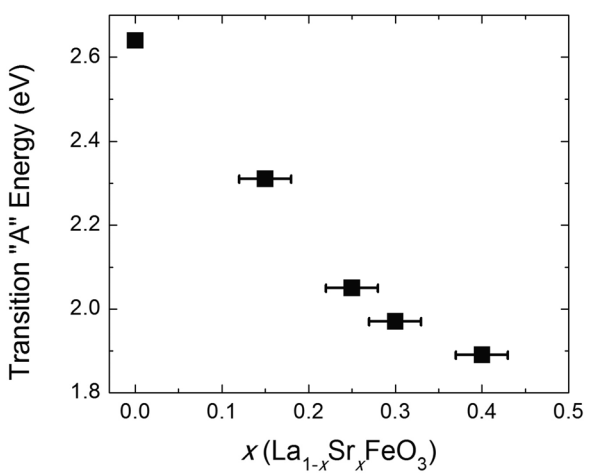

FIG. 4. The energy of transition "A" as determined from Tauc plots as a function of composition.

We note that we also attempted to model the absorption data assuming an indirect gap by plotting $(\alpha E)^{1/2}$ as a function of E; this can be seen in Supplementary Figure S2.[27] However, the results obtained from the direct gap model are in better agreement with the x-ray spectroscopy reported in Ref. 22 and the values obtained from the indirect gap for the LSFO films are at energies well into the absorption region associated with transition "C." The transition energies obtained from the indirect gap model are approximately 1 eV lower than where the absorption associated with transition "A" begins to increase. We, therefore, believe that the use of the direct gap Tauc model is more appropriate.

In conclusion, systematic changes in the optical absorption of epitaxial $La_{1-x}Sr_xFeO_3$ thin films were observed with increasing Sr content. The addition of Sr leads to a red-shifting of transitions that involve excitation to minority spin Fe $3d$ states and the formation of an additional transition at energies below the gap of LFO. These results demonstrate the feasibility of tuning electronic and optical transitions in Fe-based complex oxides within the visible spectrum using mixed valence A-site cation doping.

We thank Jenia Karapetrova, Christian Schleputz, Rebecca Sichel-Tissot, and Cole Smith for assistance with the synchrotron diffraction measurements and Caroline Schauer for access to the spectroscopic ellipsometer. S.J.M. and Y.J.X. were supported by the Office of Naval Research (N00014-11-1-0109). M.T. and J.E.S. were supported by the ARO under W911NF-08-1-0067. M.D.S. acknowledges support from the Department of Education (GAANN-RETAIN, Award No. P200A100117). X-ray diffraction was performed using the Centralized Research Facilities of the College of Engineering at Drexel University.

[1]H. Y. Hwang, Y. Iwasa, M. Kawasaki, B. Keimer, N. Nagaosa, and Y. Tokura, Nature Mater. **11**, 103 (2012).
[2]H. Kato and A. Kudo, J. Phys. Chem. B **105**, 4285 (2001).
[3]J. W. Bennett, I. Grinberg, and A. M. Rappe, J. Am. Chem. Soc. **130**, 17409 (2008).
[4]T. Choi, S. Lee, Y. J. Choi, V. Kiryukhin, and S.-W. Cheong, Science **324**, 63 (2009).

Downloaded 28 Feb 2013 to 129.25.34.167. Redistribution subject to AIP license or copyright; see http://apl.aip.org/about/rights_and_permissions

[5]S. Y. Yang, J. Seidel, S. J. Byrnes, P. Shafer, C.-H. Yang, M. D. Rossel, P. Yu, Y.-H. Chu, J. F. Scott, J. W. Ager *et al.*, Nat. Nanotechnol. **5**, 143 (2010).
[6]W. S. Choi, M. F. Chisholm, D. J. Singh, T. Choi, G. E. Jellison, Jr., and H. N. Lee, Nat. Commun. **3**, 689 (2012).
[7]Q. Liu, B. Li, J. Liu, H. Li, Z. Liu, K. Dai, G. Zhu, P. Zhang, F. Chen, and J. Dai, EPL **98**, 47010 (2012).
[8]S. Lee, W. H. Woodford, and C. A. Randall, Appl. Phys. Lett. **92**, 201909 (2008).
[9]X. Zhai, C. S. Mohapatra, A. B. Shah, J.-M. Zuo, and J. N. Eckstein, Adv. Mater. **22**, 1136 (2010).
[10]S. Lee, R. D. Levi, W. Qu, S. C. Lee, and C. A. Randall, J. Appl. Phys. **107**, 023523 (2010).
[11]X. S. Xu, J. F. Ihlefeld, J. H. Lee, O. K. Ezekoye, E. Vlahos, R. Ramesh, V. Gopalan, X. Q. Pan, D. G. Schlom, and J. L. Musfeldt, Appl. Phys. Lett. **96**, 192901 (2010).
[12]T. Arima, Y. Tokura, and J. B. Torrance, Phys. Rev. B **48**, 17006 (1993).
[13]J. Matsuno, T. Mizokawa, A. Fujimori, K. Mamiya, Y. Takeda, S. Kawasaki, and M. Takano, Phys. Rev. B **60**, 4605 (1999).
[14]J. B. Yang, W. B. Yelon, W. J. James, Z. Chu, M. Kornecki, Y. X. Xie, X. D. Zhou, H. U. Anderson, A. G. Joshi, and S. K. Malik, Phys. Rev. B **66**, 184415 (2002).
[15]E. Folven, T. Tybell, A. Scholl, A. Young, S. T. Retterer, Y. Takamura, and J. K. Grepstad, Nano Lett. **10**, 4578 (2010).
[16]S. K. Park, T. Ishikawa, Y. Tokura, J. Q. Li, and Y. Matsui, Phys. Rev. B **60**, 10788 (1999).
[17]J. Ma, J.-Q. Yan, S. O. Diallo, R. Stevens, A. Llobet, F. Trouw, D. L. Abernathy, M. B. Stone, and R. J. McQueeney, Phys. Rev. B **84**, 224115 (2011).
[18]T. Kawakami, S. Nasu, T. Sasaki, K. Kuzushita, S. Morimoto, S. Endo, T. Yamada, S. Kawasaki, and M. Takano, Phys. Rev. Lett. **88**, 037602 (2002).
[19]S. Ishiwata, M. Tokunaga, Y. Kaneko, D. Okuyama, Y. Tokunaga, S. Wakimoto, K. Kakurai, T. Arima, Y. Taguchi, and Y. Tokura, Phys. Rev. B **84**, 054427 (2011).
[20]M. Abbate, F. M. F. de Groot, J. C. Fuggle, A. Fujimori, O. Strebel, F. Lopez, M. Domke, G. Kaindl, G. A. Sawatzky, M. Takano *et al.*, Phys. Rev. B **46**, 4511 (1992).
[21]A. Chainani, M. Mathew, and D. D. Sarma, Phys. Rev. B **48**, 14818 (1993).
[22]H. Wadati, D. Kobayashi, H. Kumigashira, K. Okazaki, T. Mizokawa, A. Fujimori, K. Horiba, M. Oshima, N. Hamada, M. Lippmaa *et al.*, Phys. Rev. B **71**, 035108 (2005).
[23]H. Wadati, A. Chikamatsu, M. Takizawa, R. Hashimoto, H. Kumigashira, T. Yoshida, T. Mizokawa, A. Fujimori, M. Oshima, M. Lippmaa *et al.*, Phys. Rev. B **74**, 115114 (2006).
[24]A. Braun, D. Bayraktar, S. Erat, A. S. Harvey, D. Beckel, J. A. Purton, P. Holtappels, L. J. Gauckler, and T. Graule, Appl. Phys. Lett. **94**, 202102 (2009).
[25]O. Haas, U. Vogt, C. Soltmann, A. Braun, W.-S. Yoon, X. Yang, and T. Graule, Mater. Res. Bull. **44**, 1397 (2009).
[26]M. Bjorck and G. Andersson, J. Appl. Crystallogr. **40**, 1174 (2007).
[27]See supplementary material at http://dx.doi.org/10.1063/1.4794145 for diffraction simulations, addition Tauc plots, and obtained oscillator fitting parameters.
[28]J. W. Seo, E. E. Fullerton, F. Nolting, A. Scholl, J. Fompeyrine, and J.-P. Locquet, J. Phys.: Condens. Matter **20**, 264014 (2008).
[29]M. Kawasaki, M. Izumi, Y. Konishi, T. Manako, and Y. Tokura, Mater. Sci. Eng., B **63**, 49 (1999).
[30]H. Yamada, M. Kawasaki, and Y. Tokura, Appl. Phys. Lett. **80**, 622 (2002).
[31]T. Maeder and J. G. Bednorz, J. Eur. Ceram. Soc. **19**, 1507 (1999).
[32]A. Kumar, R. C. Rai, N. J. Podraza, S. Denev, M. Ramirez, Y.-H. Chu, L. W. Martin, J. Ihlefeld, T. Heeg, J. Schubert *et al.*, Appl. Phys. Lett. **92**, 121915 (2008).
[33]I. Marozau, A. Shkabko, M. Dbeli, T. Lippert, D. Logvinovich, M. Mallepell, C. W. Schneider, A. Weidenkaff, and A. Wokaun, Materials **2**, 1388 (2009).
[34]J. F. Ihlefeld, N. J. Podraza, Z. K. Liu, R. C. Rai, X. Xu, T. Heeg, Y. B. Chen, J. Li, R. W. Collins, J. L. Musfeldt *et al.*, Appl. Phys. Lett. **92**, 142908 (2008).

Downloaded 28 Feb 2013 to 129.25.34.167. Redistribution subject to AIP license or copyright; see http://apl.aip.org/about/rights_and_permissions